Acta Crystallographica Section B
Structural Science
ISSN 0108-7681

Relationship between structure and photoinitiating abilities of selected bromide salts of 2-oxo-2,3-dihydro-1*H*-imidazo[1,2-*a*]pyridine (IMP): influence of the solvent and the substitution in benzaldehyde on the course of its reaction with IMP

Agnieszka Plutecka,[a] Marcin Hoffmann,[a,b] Urszula Rychlewska,[a]* Zdzisław Kucybała,[c] Jerzy Pączkowski[c] and Ilona Pyszka[c]

[a]Faculty of Chemistry, Adam Mickiewicz University, Grunwaldzka 6, 60-780 Poznań, Poland, [b]BioInfoBank Institute, Limanowskiego 24A, 60-744 Poznań, Poland, and [c]Faculty of Chemical Technology and Engineering, University of Technology and Agriculture, Seminaryjna 3, 85-236 Bydgoszcz, Poland

Correspondence e-mail: urszular@amu.edu.pl

Received 20 July 2005
Accepted 19 October 2005

2-Oxo-2,3-dihydro-1*H*-imidazo[1,2-*a*]pyridinium bromide and its C3-substituted derivatives have been synthesized and structurally characterized by X-ray crystallography and quantum chemical calculations. Their potential as photoinitiators for free-radical polymerization has been investigated experimentally and compared with theoretical results. It has been established that the course of the reaction that introduces the substituted benzylidene group to the imidazole ring is different in the protic and dipolar aprotic solvents, and also depends on the character of the substituent, as the energy change in the reaction favours either $R^1R^2C{=}CHR^3$ or $R^1R^2CH{-}CH(OCH_3)R^3$ formation.

1. Introduction

As part of the program for the synthesis of dyes containing imidazopyridine (IPD) and the evaluation of their possible use as photoinitiators for free-radical polymerizations induced with the visible emission of an argon-ion laser (Pyszka *et al.*, 2003), we have been investigating the products of the reaction that introduces into 2-oxo-2,3-dihydro-1*H*-imidazo[1,2-*a*]pyridinium bromide the *ortho*- or *para*-substituted benzaldehyde derivatives.

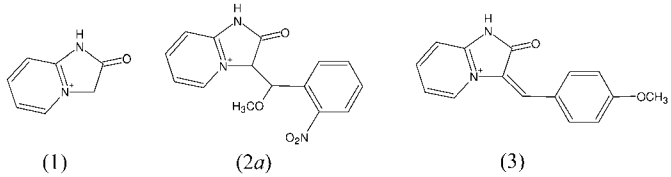

(1) (2*a*) (3)

(I)

For the molecular cations shown in (I) the crystal structures of their bromide salts have been determined by X-ray analysis and the light-absorbing abilities have been measured experimentally and calculated by quantum chemical TD-DFT (time-dependent density-functional theory) methods. The quantum chemical calculations have also been applied to estimate the energetic effect connected with the course of the hypothetical addition reaction into the benzylidene double bond.

2. Experimental

Substrates used for the preparation of the dyes, *i.e.* 4-anisaldehyde (AA), 2-nitrobenzaldehyde (NBA), 4-nitrobenzaldehyde, benzaldehyde, 2-aminopyridine (AP), ethyl bromo-

acetate (EBA), methanol (MeOH), methanol-d_4 (CD_3OD), DMSO-d_6 were purchased from Aldrich.

2.1. Synthesis

2-Oxo-2,3-dihydro-1*H*-imidazo[1,2-*a*]pyridinium bromide [IMP; (1)] was prepared using a method which has been described elsewhere (Pyszka *et al.*, 2003). The product was purified with the use of thin-layer chromatography and identified by ^{1}H and ^{13}C NMR.

2.1.1. 3-[Methoxy-(2-nitrophenyl)methyl]-2-oxo-3*H*-imidazo[1,2-*a*]pyridinium bromide (2*a*). 2-Nitrobenzaldehyde (NBA; 1.51 g, 0.01 *M*) was dissolved under magnetic stirring into 20 ml of methanol in a 50 ml round-bottom flask. Then 2-oxo-2,3-dihydro-1*H*-imidazo[1,2-*a*]pyridinium bromide (IMP; 2.15 g, 0.01 *M*) was added at room temperature. The reaction mixture was than refluxed for 1 h and cooled to room temperature. The crystals obtained were filtered and crystallized from methanol to give 1.39 g (40%) of red–brown crystals; m.p. 523–527 K. ^{1}H NMR (CD_3OD) δ 5.71, 5.91 p.p.m. (2H, HC—CHO). It should be pointed out that when the ^{1}H NMR spectrum for (2*a*) was measured in DMSO-d_6 a new signal appeared at δ = 8.90 p.p.m. (s, 1H, HC═C) at the expense of the signals at δ = 5.71 and δ = 5.91 p.p.m. observed in CD_3OD. This clearly indicates that in the dipolar aprotic solvents (2*a*) is being transformed into its benzylidene derivative (2).

2.1.2. 3-(4-Methoxybenzyliden)-2-oxo-2,3-dihydro-1*H*-imidazo[1,2-*a*]pyridinium bromide (3). A solution of 4-anisaldehyde (AA; 1.36 g, 0.01 *M*) in 20 ml of methanol was treated with 2-oxo-2,3-dihydro-1*H*-imidazo[1,2-*a*]pyridinium bromide (1) (2.15 g, 0.01 *M*). The mixture was allowed to stir under reflux for 1 h and then cooled to room temperature. The precipitate was filtered and crystallized from methanol to give 1.53 g (46%) of red–brown crystals; m.p. 525–526 K. ^{1}H NMR (DMSO-d_6) δ 3.90 (s, 3H, OCH_3), 8.50 p.p.m. (s, 1H, HC═C).

In order to place in the right perspective the mechanistic aspects of the synthesis of the dyes, in the context of acetal formation during the dissolution process of the corresponding aldehydes in methanol, four different aldehydes (2-nitrobenzaldehyde, 4-nitrobenzaldehyde, benzaldehyde and 4-anisaldehyde) were selected for further tests. These samples were mixed with MeOH (1:2 molar ratio) and the resulting mixtures were dissolved in CD_3OD. The ^{1}H NMR spectra of the reaction mixture were measured after 1 h of reaction time. It turned out that aldehydes containing the electron-withdrawing group NO_2 form acetals. This behaviour is demonstrated by the appearance of a C_{arom}—CH group, which is indicated by the ^{1}H NMR (CD_3OD) signal present in the range δ 5.60–6.05 p.p.m. [lit. ^{1}H NMR ($CDCl_3$) δ 5.35–5.95 p.p.m. (Schwarz *et al.*, 1977; Goon *et al.*, 1973; Lee & Cheng, 1997)]. The formation of acetals during the dissolution process was not observed for two other aldehydes under study, *i.e.* benzaldehyde and 4-anisaldehyde. The ^{1}H NMR measurements for 3-[methoxy-(2-nitrophenyl)methyl]-2-oxo-3*H*-imidazo[1,2-*a*]pyridinium bromide (2*a*) indicate that this compound is stable in protic MeOH or CD_3OD solvents, while the change of solvent to an aprotic one causes its transformation into (2).

The above findings permit us to conclude that the mechanistic scheme of the synthesis, and solvent-dependent properties of the dyes under study are as shown in (II*a*) and (II*b*).

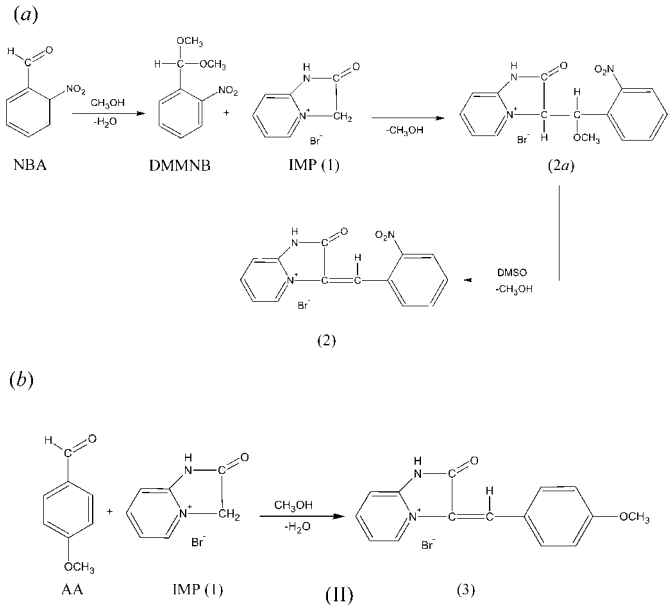

2.2. X-ray diffraction

Coloured plate-like crystals were used to measure the intensity data with a KM4CCD kappa-geometry diffractometer (*CrystAlis CCD*; Oxford Diffraction, 2000) equipped with graphite-monochromated Mo $K\alpha$ radiation (λ = 0.71073 Å). Data reduction and analysis were carried out using *CrysAlis RED* (Oxford Diffraction, 2000). The structures were solved by direct methods using *SHELXS*97 (Sheldrick, 1997*a*) and refined by least-squares techniques with *SHELXL*97 (Sheldrick, 1997*b*). The intensity data were corrected for Lp effects as well as absorption (*XEMP*; Siemens Analytical X-ray Instruments Inc., 1990). Anisotropic displacement parameters were employed for non-H atoms. In (1) the H atoms were placed at calculated positions and refined using the riding model with U_{iso}(H) = 1.2U_{iso}(C) (Sheldrick, 1990). In structures (2*a*) and (3) H-atom positions were determined from difference-Fourier maps and these H atoms were refined isotropically, except for H11 and H6 [in (2*a*)] and H2*N* [in (3)], which were treated as riding with U_{iso}(H) = 1.2U_{iso}(C) (Sheldrick, 1990). The positions of the methyl H atoms were established as follows: one of the three H atoms that constitute the methyl group was determined from a difference-Fourier map and the positions of the remaining two were calculated geometrically. All C—H(methyl) distances were standardized to a value of 0.96 Å and H-atom parameters refined using a riding model with U_{iso}(H) = 1.3U_{iso}(C) (Sheldrick, 1990). The relevant crystal

Table 1
Experimental details.

	(1)	(2*a*)	(3)
Crystal data			
Chemical formula	$C_7H_7N_2O{\cdot}Br$	$C_{15}H_{14}N_3O_4{\cdot}Br$	$C_{15}H_{13}N_2O_2{\cdot}Br$
M_r	215.06	380.20	333.18
Cell setting, space group	Triclinic, $P\bar{1}$	Monoclinic, $P2_1$	Orthorhombic, $P2_12_12_1$
a, b, c (Å)	7.2690 (10), 7.709 (2), 8.403 (2)	7.3590 (10), 12.987 (3), 8.159 (2)	8.851 (2), 10.014 (2), 15.895 (3)
α, β, γ (°)	67.01 (3), 68.03 (3), 72.00 (3)	90.00, 105.95 (3), 90.00	90.00, 90.00, 90.00
V (Å^3)	394.61 (19)	749.7 (3)	1408.8 (5)
Z	2	2	4
D_x (Mg m^{-3})	1.810	1.684	1.571
Radiation type	Mo $K\alpha$	Mo $K\alpha$	Mo $K\alpha$
No. of reflections for cell parameters	2054	2950	2956
θ range (°)	2.9–27.1	5.2–25.0	4.3–25.0
μ (mm^{-1})	5.15	2.77	2.92
Temperature (K)	295 (2)	150 (2)	295 (2)
Crystal form, colour	Planar, light brown	Plate, yellow	Cubic, light brown
Crystal size (mm)	0.4 × 0.25 × 0.1	0.4 × 0.3 × 0.08	0.4 × 0.1 × 0.1
Data collection			
Diffractometer	Kuma KM4CCD κ-geometry	Kuma KM4CCD κ-geometry	Kuma KM4CCD κ-geometry
Data collection method	ω scans	ω scans	ω scans
Absorption correction	Multi-scan (based on symmetry-related measurements)	Multi-scan (based on symmetry-related measurements)	Multi-scan (based on symmetry-related measurements)
T_{min}	0.234	0.381	0.543
T_{max}	0.592	0.801	0.750
No. of measured, independent and observed reflections	4519, 1707, 1527	3720, 1957, 1759	10 831, 2472, 1972
Criterion for observed reflections	$I > 2\sigma(I)$	$I > 2\sigma(I)$	$I > 2\sigma(I)$
R_{int}	0.035	0.034	0.091
θ_{max} (°)	27.1	25.0	25.0
Range of h, k, l	$-7 \Rightarrow h \Rightarrow 9$ $-9 \Rightarrow k \Rightarrow 9$ $-10 \Rightarrow l \Rightarrow 10$	$-8 \Rightarrow h \Rightarrow 8$ $-15 \Rightarrow k \Rightarrow 12$ $-7 \Rightarrow l \Rightarrow 9$	$-10 \Rightarrow h \Rightarrow 7$ $-11 \Rightarrow k \Rightarrow 11$ $-18 \Rightarrow l \Rightarrow 18$
Refinement			
Refinement on	F^2	F^2	F^2
$R[F^2 > 2\sigma(F^2)]$, $wR(F^2)$, S	0.020, 0.050, 1.02	0.028, 0.052, 0.96	0.047, 0.117, 0.98
No. of reflections	1707	1957	2472
No. of parameters	101	244	217
H-atom treatment	Constrained to parent site	Mixture of independent and constrained refinement	Refined independently
Weighting scheme	$w = 1/[\sigma^2(F_o^2) + (0.0288P)^2]$, where $P = (F_o^2 + 2F_c^2)/3$	$w = 1/[\sigma^2(F_o^2) + (0.0242P)^2]$, where $P = (F_o^2 + 2F_c^2)/3$	$w = 1/[\sigma^2(F_o^2) + (0.0716P)^2]$, where $P = (F_o^2 + 2F_c^2)/3$
$(\Delta/\sigma)_{max}$	0.001	< 0.0001	0.001
$\Delta\rho_{max}$, $\Delta\rho_{min}$ (e Å^{-3})	0.25, −0.37	0.42, −0.33	0.56, −0.89
Extinction method	*SHELXL*	None	None
Extinction coefficient	0.022 (3)	–	–
Absolute structure	–	Flack (1983)	Flack (1983)
Flack parameter	–	0.001 (9)	−0.022 (18)

Computer programs used: *CrysAlisCCD* (Oxford Diffraction, 2000), *CrysAlisRED* (Oxford Diffraction, 2000), *SHELXS*97 (Sheldrick, 1990), *SHELXL*97 (Sheldrick, 1997*b*); Siemens Analytical X-ray Instruments, 1989).

data collection and refinement parameters are listed in Table 1.

2.3. Quantum chemical calculations

The structures observed in the crystals were used as starting points for DFT (density functional theory) full-geometry optimization for the isolated molecular cations. The structures were optimized using the hybrid functional – B3LYP (Becke, 1993; Parr & Yang, 1989) method (Becke's three-parameter functional with the Lee–Yang–Parr exchange–correlation potential; Lee *et al.*, 1988) – at the split-valence double ζ 6-31+G(d) basis sets (6-31G basis set augmented with polarization and diffuse functions; Ditchfield *et al.*, 1971; Hehre *et al.*, 1972; Gordon, 1980; Hariharan & Pople, 1973, 1974; Clark *et al.*, 1983; Frisch *et al.*, 1984). Having optimized geometries for the studied systems (geometrical parameters for these structures are listed in Tables 1aS and 1bS of the supplementary data[1]), time-dependent (TD) DFT calculations (Bauernschmitt & Ahlrichs, 1996; Casida *et al.*, 1998; Stratmann *et al.*, 1998) were performed in order to calculate the oscillator strengths, transition dipole moments and excitation

[1] Supplementary data for this paper are available from the IUCr electronic archives (Reference: GP5003). Services for accessing these data are described at the back of the journal.

energies for (1), (2), (2*a*), (3) and (3*a*) [see (I) and (III)]. The results are listed in Table 2. All calculations were carried out with the *GAUSSIAN*03 (Frisch *et al.*, 2003) program in the Poznań Supercomputing and Networking Center.

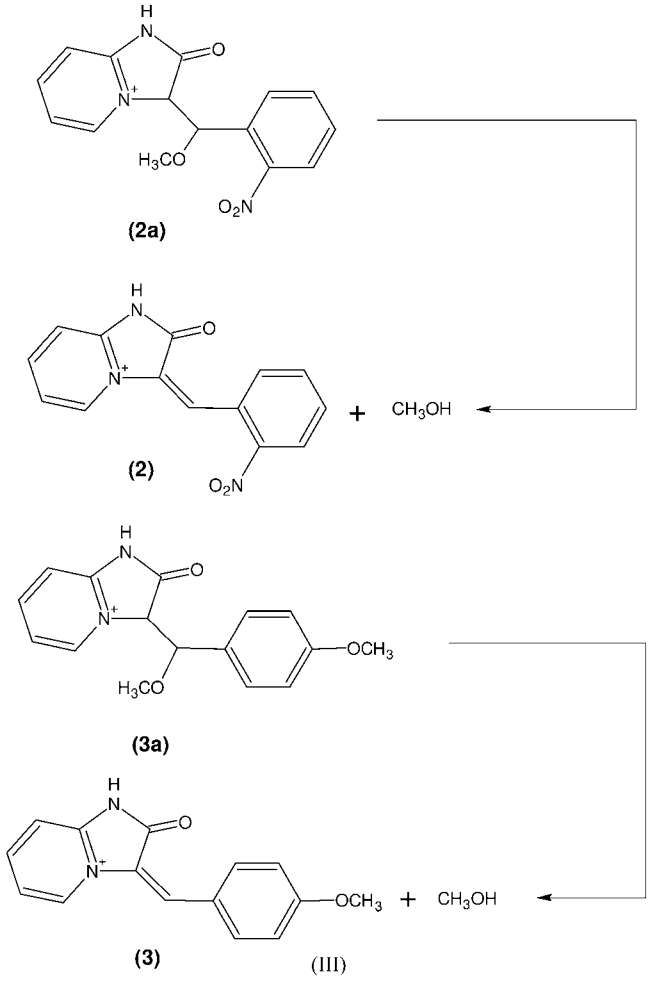

To shed some light on the factors favouring the carbon–carbon double bond for (3), but its saturation in (2*a*), energies were calculated for the corresponding systems: (3*a*) – obtained after methanol addition to (3); (2) – obtained after methanol elimination from (2*a*). The (3*a*) and (2) structures were optimized at the same level of theory as the systems of (1), (2*a*) and (3). In order to make up for basis-set superposition error the counterpoise correction procedure (Boys & Bernardi, 1970; Simon *et al.*, 1996) was applied for the (2*a*) and (3*a*) species. Owing to the various assumptions and simplifications in the utilized computational methods, the energetic effect for the reaction of methanol elimination and the benzylidene carbon–carbon double-bond formation was calculated as the energy difference between the reactants and products.

3. Results and discussion

3.1. Geometric and electronic structure

The parent compound and the products of its reaction with substituted benzaldehyde have been obtained in the form of bromide salts (1), (2*a*) and (3), respectively. Drawings presenting the content of the independent part of the unit cell for the three investigated crystal structures are shown in Fig. 1. As illustrated in Fig. 1, the presence of an electron-withdrawing substituent in the *ortho*-position [the nitro-group, compound (2*a*)] obstructs the formation of the benzylidene double bond in the course of the reaction of 2-nitrobenzaldehyde with IMP. This is because the dissolution of 2-nitrobenzaldehyde in methanol proceeds *via* the formation of acetal (see above). Consequently, the molecule gains two chirality centers (at C6 and C8). In contrast to this, in the presence of an electron-donating group in the *para* position

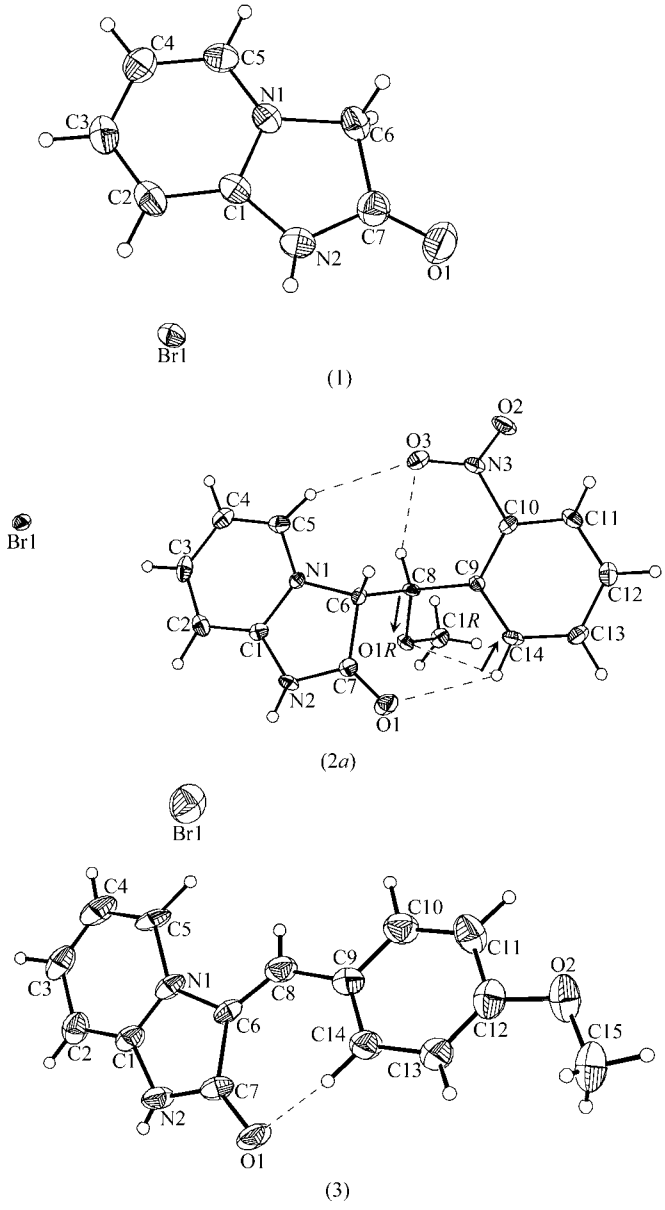

Figure 1
Displacement ellipsoid representation (40% probability level) of the asymmetric part of the unit cell and atom-numbering scheme for (1), (2*a*) and (3), respectively. The H atoms are drawn as spheres of arbitrary size. Arrows mark local CO and CH dipoles. Intramolecular hydrogen bonds are denoted by dashed lines.

Table 2
Excitation energies and oscillator strengths obtained from TD B3LYP/6-31+G(d) calculations for the HOMO–LUMO excitation and corresponding experimental data.

Excitation energy and oscillator strength measured in CH_3OH.

	Calculated data		Experimental results			
Compound	Excitation energy (nm)	Oscillator strength	Excitation energy (nm)	Oscillator strength	Reduction potential (mV)	Photoinitiation ability (μmol s^{-1})
(1)	285	0.101	307	0.115	–	–
(2*a*)	342	0.026	308	0.038	–	–
(2)	385	0.477	455†	0.36†	−1128‡	1.54
(3)	433	0.792	419	0.567	−1228‡	1.78
(3*a*)	616	0.060	–	–	–	–

† Measured in DMSO. ‡ Measured in MeCN.

Table 3
Hydrogen-bond parameters (Å, °).

Compund	Hydrogen bond	H···*A*	*D*···*A*	*D*—H···*A*
(1)	C6—H6*B*···O1^{i}	2.56	3.200 (3)	124
	N2—H2*A*···Br1^{ii}	2.45	3.221 (2)	161
(2*a*)	C5—H5···O3	2.52 (3)	3.351 (6)	154 (4)
	C8—H8···O3	2.36 (3)	2.850 (5)	112 (3)
	C14—H14···O1	2.64 (4)	3.115 (6)	114 (3)
	C14—H14···O1*R*	2.58 (4)	2.877 (5)	100 (3)
	C2—H2···O2^{iii}	2.40 (4)	3.255 (6)	151 (4)
	C1*R*—H3*R*···O2^{iv}	2.45	3.274 (5)	149
	N2—H2*A*···Br1^{v}	2.49 (4)	3.296 (4)	170 (4)
(3)	C14—H14···O1	2.20 (6)	3.005 (7)	145 (5)
	N2—H2*N*···Br1^{vi}	2.39	3.195 (4)	169
	C4—H4···O1^{vii}	2.38 (5)	3.132 (6)	148 (5)
	C11—H11···O1^{viii}	2.76 (6)	3.457 (7)	137 (5)

Symmetry codes: (i) $1-x, 1-y, 2-z$; (ii) $x, -1+y, 1+z$; (iii) $2-x, -\frac{1}{2}+y, 1-z$; (iv) $3-x, -\frac{1}{2}+y, 2-z$; (v) $-1-x, -\frac{1}{2}+y, 1-z$; (vi) $-\frac{1}{2}+x, \frac{1}{2}-y, 2-z$; (vii) $1+x, y, z$; (viii) $1-x, \frac{1}{2}+y, \frac{3}{2}-z$.

[the methoxy group, compound (3)], the benzylidene double bond is formed. The bond lengths, valence angles and net charges for atoms in molecules (1), (2*a*) and (3) are listed in Tables 2aS, 2bS and 3S, respectively.

An analysis of the geometry and electronic structure of the parent compound (1) allows us to propose a resonance structure, as shown in (I). This electronic structure is different from the three tautomeric forms proposed previously on the basis of the X-ray analysis of the chloride salt (Rybakov *et al.*, 2000) of (1). As far as the geometry of IMP is concerned, noticeable differences between the two salts are seen within the pyridine moiety.

In all three investigated compounds, the imidazopyridine moieties are roughly planar with overall root-mean-square deviations (r.m.s.d.) for the ring atoms of 0.011 (1), 0.034 (3) and 0.010 (4) Å, for (1), (2*a*) and (3), respectively, although a slight puckering towards the C7 envelope conformation is oberved in (2*a*). The IMP moiety, common to the three investigated molecules, has similar geometry. (Interatomic distances and angles are listed in Tables 2aS and 2bS1, respectively.) However, some changes appear as a result of dehydrogenation at the C6 atom in (3): nearly all the bonds in the imidazole ring of (3) become shorter, indicating higher electron delocalization within this ring compared with the parent compound. At the same time, the carbonyl bond becomes significantly longer and, parallel to this, we observe an increase in the net atomic charges on atoms constituting the C=O group. The two effects are consistent with the higher polarization of this bond. There is also a dramatic change of the net atomic charge at C6 [from distinctively negative, −0.35 e, in the parent compound (1), to nearly neutral, −0.02 e, in (3)]. The net atomic charges for atoms, calculated by NPA (Carpenter & Weinhold, 1988; Foster & Weinhold, 1980; Reed & Weinhold, 1983; Reed *et al.*, 1985, 1988) and Mulliken (Mulliken, 1955) population analyses, are listed in Table 3S1.

Higher electron delocalization within the imidazole ring in (3) compared with (1) and (2*a*), and combined with it an increase of the aromatic character of this ring, might also be a result of the presence of the so-called resonance-assisted intramolecular hydrogen bond between the C—H(phenyl) group as a donor and the imidazole carbonyl group as an acceptor (C14—H14···O1). The hydrogen-bond parameters are listed in Table 3.

The phenyl rings in (2*a*) and (3) are planar, the r.m.s.d.'s for these rings being 0.007 (3) and 0.003 (4) Å, respectively. The nitro group in (2*a*) is significantly twisted out of the phenyl ring by 40.2 (2)°. The severe twisting of the *ortho*-nitro group out of the ring plane in (2*a*) most likely arises from the need to relieve steric crowding with the substituents at C8, *i.e.* the IMP moiety and the methoxy group. A database study (Allen, 1998, 2002; Allen *et al.*, 1979; Allen & Kennard, 1993) of nitrophenyls *ortho*-substituted with a sp^3 hybridized C atom found an average twist angle of 31.9° with a standard deviation of 13.8° (n = 70, n is the number of observations). When the hybridization of the *ortho*-substituted C atom has not been specified, the number of observations significantly increased to n = 184, resulting in an almost identical value of the mean twist angle of 31.5 (16.6)°. However, for nitro groups with two H atoms in the position *ortho* to the nitro group, a nearly coplanar arrangement with the benzyl ring is favoured (average twist angle of 7.7° with a sample standard deviation of 6.0° for n = 6124). Clearly, steric effects play a dominant role in the geometry of the *ortho* nitro derivatives. Moreover, a severe twisting of the nitro group out of the phenyl ring plane in (2*a*) enables the formation of an intramolecular hydrogen bond between one of its O atoms serving as an acceptor and the *ortho*-positioned C—H group (C8—H8···O3; Table 3). A list of the intramolecular hydrogen bonds present in (2*a*) should be extended to three other C—H···O interactions with O atoms belonging to the nitro, carbonyl and methoxy groups (C5—H5···O3, C14—H14···O1 and C14—H14···O1*R*, respectively, Table 3). All these intramolecular hydrogen-bond interactions are presumably responsible for a relatively co-planar arrangement of the imidazopyridine and phenyl rings, the angle between them being only 12.2 (1)°. The latter

C—H···O1*R* interaction, classified as a very weak hydrogen bond (methoxy O atoms are known as poor acceptors), should, in our opinion, be considered as an attractive interaction between antiparallel local dipoles formed along C8—O1*R* and C14—H14 bonds. The separation of point charges calculated from NPA for C8—O1*R* is 0.69 e (oxygen more negative), while for C14—H14 it is 0.48 e (carbon more negative). The angle between these two vectors is 153°, which is close to 180°, the ideal antiparallel arrangement. We have already oberved such intramolecular interactions in a series of tartaric acid derivatives (Rychlewska & Warżajtis, 2001; Rychlewska *et al.*, 1997; Gawroński *et al.*, 1997). The proximity of the two oxygen atoms O1 and O1*R* additionally polarizes the C14—H14 bond, thus creating favourable conditions for this kind of electrostatic interaction.

Contrary to the *ortho* nitro group in (2*a*), the *para*-methoxy group in (3) lies in the plane of the benzyl ring, with the twist angle being only 1.9 (8)°. The database search carried out for *para*-methoxybenzylidenes found an H3C—O—CBz—CBz torsion angle of 4.6° with a standard deviation of 3.4 ° for 117 observations (the torsion angle magnitudes were restricted to lie in the range 0–90°). The presence of only one intramolecular hydrogen bond in (3) compared with three such bonds in (2*a*) (Table 3) influences the mutual orientation of the imidazopyridine and methoxyphenyl moieties. The two rings form an interplanar angle of 22.5 (2) °, which is significantly larger than that in (2*a*) [12.2 (1)°; see above].

It has been known for quite some time (Carter *et al.*, 1966) that within the benzene ring the valence angles at the C atoms bearing substituents with strong electron-withdrawing power are significantly larger than 120°. Likewise, at C atoms bearing strong electron-releasing substituents, the angles are consistently less than 120°. In (2*a*) the electron-withdrawing nitro group at the *ortho* position, carrying, according to Mulliken population analysis, an overall negative charge of −0.395 e (Table 3S1), is responsible for an increase of the C9—C10—C11 angle to 123.4 (4)°. In (3) where the substituent at the *para* position is electron-releasing, the overall charge for the methoxy group has been calculated as +0.004 e and the valence angle at the substituted carbon is 121.2 (5)°, not significantly different from 120°. Likewise, protonation at N2 is responsible for widening the C1—N2—C7 valence angle within the five-membered imidazoline ring to the values of 112.5 (4), 112.4 (1) and 111.2 (4)° in (1), (2*a*) and (3), respectively.

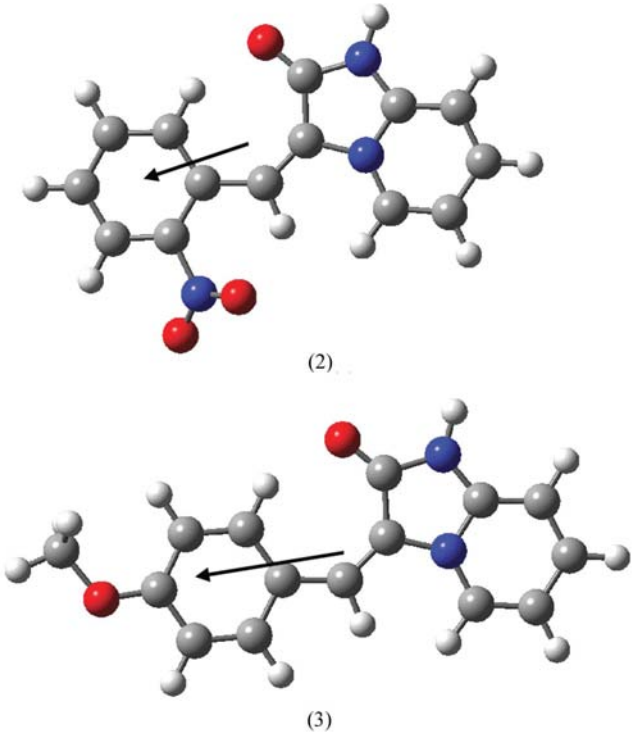

Figure 2
Transition electric dipole moments for (2) and (3) plotted against the molecules. Origin of the vector chosen arbitrary.

3.2. Photoinitiating abilities of the studied compounds

TD-DFT calculations were utilized to assess the excitation energies and oscillator strengths for (1), (2*a*), (2), (3) and (3*a*). In the case of (1), (2), (2*a*) and (3) the theoretically calculated values were compared with those obtained from experimental measurements. Table 2 summarizes the results from TD-DFT calculations, while Fig. 2 graphically presents the transition electric dipole moments for (2) and (3).

As is obvious from Table 2, the calculated and measured oscillator strengths are in good agreement. The highest oscillator strengths were obtained for (2) and (3), which possess the benzylidene carbon–carbon double bond. However, comparison between (2) and (3) reveals that molecule (3), having the methoxy substituent in the *para* position in the phenyl ring, is a far better photoinitiator (oscillator strength of 0.567 measured and 0.792 calculated) than molecule (2), which has a nitro substituent in the *ortho* position (oscillator strength of 0.36 measured and 0.477 calculated). Not surprisingly, the molecules without a benzylidene carbon–carbon double bond, *i.e.* (1), (2*a*) and (3*a*), are much poorer photoinitiators with oscillator strengths lower than 0.1.

3.3. Energetic effect associated with the formation of the benzylidene double bond upon elimination of methanol

In order to estimate the energetic effect associated with the elimination of methanol and the subsequent formation of the benzylidene double bond, we have calculated at the B3LYP/6-31+G(d) level the energies of the systems possessing a carbon–carbon double bond [(2) and (3)], as well as the systems before methanol elimination [(2*a*) and (3*a*)]. The computationally studied molecular cations and the reactions connecting the species are shown in (III). Table 4 presents the energy differences, both counterpoise corrected and uncorrected, between the reactants and products for the methanol elimination reaction.

The energetic effect of the reaction disfavours the elimination of methanol from (2*a*) and the formation of (2), as the product is higher in energy than the reactants. Counterpoise corrected results indicate that (2*a*) is −58.6 kJ mol^{-1} lower in

Table 4
Energetic effects associated with the elimination of methanol.

Reaction	ΔE (kJ mol^{-1})	ΔE (kJ mol^{-1}) counterpoise corrected
(2*a*) → (2) + MeOH	71	58
(3*a*) → (3) + MeOH	8	−12

energy, while uncorrected that it is of −71.2 kJ mol^{-1} lower in energy. In the case of the reaction connecting (3) and (3*a*), the situation is the opposite. Counterpoise corrected results indicate that product (3) and methanol are slightly (of 12.6 kJ mol^{-1}) lower in energy than the reactant (3*a*). The uncorrected results favour the formation of (3*a*) by 8.4 kJ mol^{-1}. These calculated energy differences elucidate well the reason why, despite the same procedure being applied in the synthesis of (2*a*) and (3), one obtains two different types of product. Namely, in the case of the compound bearing the *para*-methoxy group one obtains a product containing the benzylidene double bond, while for the compound possessing the *ortho* NO_2 group the methanol addition occurs.

3.4. Packing and hydrogen bonding

The list of hydrogen bonds in the investigated crystal structures is presented in Table 3. In all the crystal structures reported the imidazole N—H group acts as a hydrogen-bond donor and the bromide anion as an acceptor, thus forming the so-called charge-assisted (Jeffrey, 1999) hydrogen bond. As there are no other strong hydrogen-bond donors, the remaining hydrogen bonds are of the C—H···O type. In the parent compound (1) the only possible C—H···O bond, located over a long distance range (2.56 Å), deviates significantly from linearity (124°) and involves the Csp^3 atom as a donor, therefore, it is a very weak interaction. In the nitro derivative (2*a*), the H···O separations are in the range 2.36 (3)–2.65 (4) Å and lie within the range specified by Steiner 2.22–2.62 Å (Steiner, 2002). Both nitro O atoms are involved simultaneously in two hydrogen bonds, but one of them (O3) is involved solely in intramolecular hydrogen bonds, while the other (O2) exclusively in intermolecular interactions. Interestingly, the carbonyl O atom attached to the imidazole ring is involved solely in a very weak intramolecular interaction with H14. In line with this observation is a very short C=O bond [1.198 (5) Å], but the net atomic charge on this O atom is comparable with that observed in the parent compound (1).

Compared with the crystal structures of (1) and (2*a*), the involvement of the carbonyl oxygen in hydrogen-bond formation in (3) seems to be much stronger. O1 accepts two inter- and one intramolecular hydrogen bond. The latter interaction, which seems rather strong, is presumably responsible for the significant elongation of the carbonyl bond [1.229 (5) Å] and a significant increase of the point-charge separation within the carbonyl group. For NPA the negative point charge condensed on the O atom increases from −0.487 to −0.510 e and the positive charge on the C atom from +0.682 to +0.706 e (Table 3S). The observed intramolecular hydrogen bond belongs to the so-called resonance-assisted hydrogen bonds (Gilli *et al.*, 1989; Bertolasi *et al.*, 1991).

4. Conclusions

It appears that there exists a relationship between the position and the character of the substituent in benzaldehyde, and the product of its reaction with 2-oxo-2,3-dihydro-1*H*-imidazo[1,2-*a*]pyridinium bromide. The presence of an electron-withdrawing nitro group in the *ortho* position facilitates acetal formation at the first step of the reaction and hinders subsequent methanol elimination in protic solvents, thus obstructing the formation of the benzylidene double bond. On the other hand, the presence of an electron-donating methoxy group at the *para* position leads to the appropriate benzylidene derivative. It has been demonstrated, both experimentally and theoretically, that benzylidene derivatives possess higher photoinitiating ability than their benzyl analogues. Moreover, the electron-donating substituent (OCH_3) in the *para* position in the phenyl ring leads to much higher oscillator strengths than an electron-accepting substituent (NO_2) in the *ortho* position. An energetic effect associated with the elimination of methanol and the subsequent formation of the benzylidene double bond has been estimated by DFT methods as being positive in the case of *para*-methoxy benzylidene and negative in the case of *ortho*-nitro benzylidene. The presence of various intramolecular interactions, including hydrogen bonds of the C—H···O type and the dipolar interaction between CO/βCH local dipoles, may explain the relatively high co-planarity of the imidazopyridyl and phenyl rings in (2*a*).

This work was partially financed during the years 2003–2006 by the Polish State Committee for Scientific Research as the scientific project No 4-T09A 185 25 and 3-T09B 124 26. The authors thank the Poznań Supercomputing and Networking Center for access to computer resources therein.

References

Allen, F. H. (1998). *Acta Cryst.* A**54**, 758–771.
Allen, F. H. (2002). *Acta Cryst.* B**58**, 380–388.
Allen, F. H., Bellard, S., Brice, M. D., Cartwright, B. A., Doubleday, A., Higgs, H., Hummelink, T., Hummelink-Peters, B. G., Kenndard, O., Motherwell, W. D. S., Rodgers, J. R. & Watson, D. G. (1979). *Acta Cryst.* B**35**, 2331–2339.
Allen, F. H. & Kennard, O. (1993). *Chem. Des. Autom. News*, **8**, 1, 31–37.
Bauernschmitt, R. & Ahlrichs, R. (1996). *Chem. Phys. Lett.* **256**, 454–464.
Becke, A. D. J. (1993). *J. Chem. Phys.* **98**, 5648–5652.
Bertolasi, V., Gilli, P., Ferretti, V. & Gilli, G. (1991). *J. Am. Chem. Soc.* **113**, 4917–4925.
Boys, S. F. & Bernardi, F. (1970). *Mol. Phys.* **19**, 553–571.
Carpenter, J. E. & Weinhold, F. (1988). *J. Mol. Struct. Theochem.* **169**, 41–62.
Carter, O. L., McPhail, A. T. & Sim, G. A. (1966). *J. Chem. Soc. A*, pp. 822–838.
Casida, M. E., Jamorski, C., Casida, K. C. & Salahub, D. R. (1998). *J. Chem. Phys.* **108**, 4439–4449.

Clark, T., Chandrasekhar, J., Spitznagel, G. W. & Schleyer, P. R. (1983). *J. Comput. Chem.* **4**, 294–301.
Ditchfield, R., Hehre, W. J. & Pople, J. A. (1971). *J. Chem. Phys.* **54**, 724–728.
Flack, H. D. (1983). *Acta Cryst.* A**39**, 876–881.
Foster, J. P. & Weinhold, F. (1980). *J. Am. Chem. Soc.* **102**, 7211–7218.
Frisch, M. J., Pople, J. A. & Binkley, J. S. (1984). *J. Chem. Phys.* **80**, 3265–3269.
Frisch, M. J. *et al.* (2003). *GAUSSIAN*03, Revision B.05. Gaussian, Inc., Pittsburgh PA, USA.
Gawroński, J., Gawrońska, K., Skowronek, P., Rychlewska, U., Warżajtis, B., Rychlewski, J., Hoffmann, M. & Szarecka, A. (1997). *Tetrahedron*, **53**, 6113–6144.
Gilli, G., Bellucci, F., Ferretti, V. & Bertolasi, V. (1989). *J. Am. Chem. Soc.* **111**, 1023–1028.
Goon, D. J. W., Murray, N. G., Schoch, J. P. & Bunce, N. J. (1973). *Can. J. Chem.* **51**, 3827–3832.
Gordon, M. S. (1980). *Chem. Phys. Lett.* **76**, 163–168.
Hariharan, P. C. & Pople, J. A. (1973). *Theor. Chim. Acta*, **28**, 213–222.
Hariharan, P. C. & Pople, J. A. (1974). *Mol. Phys.* **27**, 209–214.
Hehre, W., Ditchfield, R. & Pople, J. A. (1972). *J. Chem. Phys.* **56**, 2257–2261.
Jeffrey, G. A. (1999). *An Introduction to Hydrogen Bonding.* New York: Oxford University Press.
Lee, A. S. Y. & Cheng C. L. (1997). *Tetrahedron*, **53**, 14255–14262.
Lee, C., Yang, W. & Parr, R. G. (1988). *Phys. Rev. B*, **37**, 785–789.
Mulliken, R. S. (1955). *J. Chem Phys.* **23**, 1833–1840.
Oxford Diffraction (2000). *CrystAlis CCD Software*, Version 1.171. Oxford Diffraction, Oxfordshire, England.
Parr, R. G. & Yang, W. (1989). *Density-Functional Theory of Atoms and Molecules.* New York: Oxford University Press.
Pyszka, I., Kucybała, Z. & Pączkowski, J. (2003). *J. Polym. Sci. Part A*, **41**, 3048–3055.
Reed, A. E., Curtiss, L. A. & Weinhold, F. (1988). *Chem. Rev.* **88**, 899–926.
Reed, A. E. & Weinhold, F. (1983). *J. Chem. Phys.* **78**, 4066–4073.
Reed, A. E., Weinstock, R. B. & Weinhold, F. (1985). *J. Chem. Phys.* **83**, 735–746.
Rybakov, V. B., Znukov, S. G., Babaev, E. V., Mazina, O. S. & Aslanov, L. A. (2000). *Kristallografiya*, **45**, 108–110.
Rychlewska, U. & Warżajtis, B. (2001). *Acta Cryst.* B**57**, 415–427.
Rychlewska, U., Warżajtis, B., Hoffmann, M. & Rychlewski, J. (1997). *Molecules*, **2**, 106–113.
Schwarz, H., Sezi, R., Levsen, K., Heimbach, H. & Borchers, F. (1977). *Org. Mass Spectrom.* **12**, 569–572.
Sheldrick, G. M. (1990). *Acta Cryst.* A**46**, 467–473.
Sheldrick, G. M. (1997*a*). *SHELXS*97. University of Göttingen, Germany.
Sheldrick, G. M. (1997*b*). *SHELXL*97. University of Göttingen, Germany.
Siemens Analytical X-ray Instruments Inc. (1990). *XEMP*, Version 4.2. Siemens Analytical X-ray Instruments Inc., Madison, Wisconsin, USA.
Simon, S., Duran, M. & Dannenberg, J. J. (1996). *J. Chem. Phys.* **105**, 11024–11031.
Steiner, T. (2002). *Angew. Chem. Int. Ed.* **41**, 48–76.
Stratmann, R. E., Scuseria, G. E. & Frisch, M. J. (1998). *J. Chem. Phys.* **109**, 8218–8224.